Published in Helvetica Chimica Acta, vol. 92, 2009, p. 2173-2185 (Wiley-VCH

Multiple Frequency and Variable Temperature EPR study of Gd(III) polyaminocarboxylates: analysis and comparison of the magnetically dilute powder and the frozen solution spectra

by **Meriem Benmelouka**[a)], **Johan Van Tol**[b)], **Alain Borel** [a)], **Saritha Nellutla**[b)], **Marc Port**[d)], **Lothar Helm***[a)], **Louis-Claude Brunel**[b)c)], **and André E. Merbach**[a)]

[a)] Institut des Sciences et Ingénierie Chimiques, Ecole Polytechnique Fédérale de Lausanne, EPFL-BCH, CH-1015 Lausanne, Switzerland (fax : +41-21-6939895, email: lothar.helm@epfl.ch)

[b)] National High Magnetic Field Laboratory, Center for Interdisciplinary Magnetic Resonance, Florida State University, Tallahassee, Florida, USA

[c)] Present address: Center for Terahertz Science and Technology, Department of Physics, University of California, Santa Barbara, CA, USA

[d)] Guerbet, Research Department, 95943 Roissy Cdg Cedex, France

Dedicated to Prof. Jean-Claude Bünzli on the occasion of his 65th birthday in recognition of his prominent contribution to lanthanide chemistry

Corresponding author:
Prof. Lothar Helm
Ecole Polytechnique Fédérale de Lausanne (EPFL)
Institut des Sciences et Ingénierie Chimiques
EPFL-BCH
CH-1015 Lausanne (Switzerland)
Fax: (+41) 21-693-9895
E-mail: lothar.helm@epfl.ch

ABSTRACT

An Electron Paramagnetic Resonance (EPR) study of glasses and magnetically dilute powders of $[Gd(DTPA)(H_2O)]^{2-}$, $[Gd(DOTA)(H_2O)]^{-}$, and macromolecular Gd-P792 complexes was carried out at X-, Q-band and 240 GHz. The results show that the zero-field splitting parameters for these complexes are quite different in a powder as compared to the frozen aqueous solution. In several complexes an inversion of the sign of the axial component *D* of the zero field splitting is observed, indicating a significant structural change. In contrary to what has been expected, powder sample do not allow a more precise determination of the static ZFS parameters in the powders obtained by liophilization. The results obtained in glasses are more relevant to the problem of electron spin relaxation in aqueous solution than those obtained from powders.

KEYWORDS

MRI, Gd(III) complexes, Contrast Agents, Multiple-frequency EPR, magnetically dilute powders.

Introduction. - In recent years Magnetic Resonance Imaging has evolved into one of the most powerful diagnostic techniques in medicine, in part thanks to the application of suitable contrast agents. These paramagnetic pharmacological compounds function by increasing the relaxation rate of water protons in the surrounding tissue, due to the interaction of the proton spins with the electron spin of the complex. The majority of the currently used contrast agents are thermodynamically and kinetically stable gadolinium(III) chelates. This trivalent lanthanide ion has the highest possible number (seven) of unpaired electrons which makes it the most paramagnetic among the non radioactive metal ions. The slow relaxation of the Gd(III) electron spin is an additional critical factor. The design of new, more efficient MRI contrast media requires a thorough understanding of all factors and mechanisms that influence relaxation enhancement of proton nuclear spins (relaxivity), and hence the efficiency of Gd(III) complexes [1].

Among other factors, the relaxivity is determined by (1) the rotational diffusion of the complex, described by a correlation time τ_R, (2) the chemical exchange of the water molecules directly bound to the metal with bulk water molecules (residence time τ_m), and (3) the electronic spin relaxation times T_{1e} and T_{2e}. While the molecular factors influencing (1) and (2) are rather well understood [2-5], the electronic spin relaxation of Gd(III) complexes relevant for MRI remains the subject of much discussion [6-15].

A general model for electronic relaxation of Gd(III) complexes in solution was presented by Rast et al [8] where the electron spin dynamics is determined by the rotation of a so-called static zero-field splitting (ZFS) and a modulation of a transient ZFS by random Brownian rotation of the complex and collisions with solvent molecules, respectively. Experimental EPR peak to peak line widths of several Gd(III) complexes were extracted from systematic measurements at variable temperature (0-100°C), concentration and frequency (9.44, 35, 75, 150, 225 GHz) [9]. The data were interpreted using static ZFS parameters at second, fourth and sixth order and a transient ZFS parameter at second order. While this improvement in theory is exciting, it contains a large number of parameters: four parameters for the amplitude of ZFS, two correlation times and two activation energies describing their temperature

dependence. An independent measurement of ZFS parameters will be useful. Rast's model describes the transient ZFS modulation using an Ornstein-Uhlenbeck process [16], namely random jumps around an average value with a Gaussian probability distribution. This process is actually a dynamical equivalent to the *strain* encountered in the analysis of disordered solid-state EPR spectra [17, 18]. Gaussian strain is a phenomenological description of a distribution of the spin Hamiltonian parameters throughout the sample, for example due to differences in the hydrogen bonding pattern around the spins. This model can be applied to the *g*-factor [19-21] (*g*-strain) and hyperfine coupling [22, 23] (*A*-strain), as well as to the ZFS tensor [24-26] (*D*, *E*-strain). Therefore, the determination of the ZFS parameters and their associated strains in the solid state provides us with an independent access to the key factors governing electron spin relaxation in Gd(III) complexes.

In addition to its importance in the context of multiple-frequency methods, high frequency EPR (ν > 90 GHz) has a unique application as a single frequency observation. In a previous study of frozen solutions of Gd-complexes we have shown that measurements at very high frequency (240GHz) and very low temperature (T = 4 K) allow to obtain values for the four parameters of the ZFS (D, E, σD and σE). Furthermore, the technique allowed to determine directly from the EPR spectra the sign of the axial component D for the chelating ligands studied: $D > 0$ for acyclic and $D < 0$ for cyclic [27]. Experimental spectra of frozen solutions at higher temperatures could be simulated with the parameters determined at 4 K.

In this paper, we first show that EPR spectra of frozen solutions at lower frequencies (X- and Q-band) can also be successfully simulated with the 4K, 240 GHz determined parameters. With the aim to determine more precisely the magnitude of the static ZFS by reducing as much as possible the transient component -which means strain-, we extend this EPR study to magnetically dilute powders of the DOTA- and DTPA-complexes and two macromolecular DOTA-derivatives of the Gd-P792 family: Complex (R) with six different stereoisomers determined by the configuration at each of the stereogenic centers at carbon: 4*R* (4*S*); *RSSS* (*SRRR*) and the achiral diastereoisomers *RSRS* and *RRSS* and complex

(B) with the configuration 4*R* (4*S*) (*Scheme 1*) at X-, Q-band, and at 240 GHz. In the case of the powders and as our working hypothesis the strain is supposed to be largely reduced.

Experimental. – 1. *Materials.* The DTPA and the DOTA ligands were purchased from Sigma-Aldrich and used without further purification. The Gd-P792 (R, B) powders were supplied from Guerbet pharmaceuticals.

2. *Samples preparation.* Solution of $[Gd(DTPA)(H_2O)]^{2-}$ and $[Gd(DOTA)(H_2O)]^{-}$ were prepared *in situ* by dissolution of the ligand (10% excess) in a $Gd(ClO_4)_3$ solution. The pH was adjusted to 6.5 by adding NaOH solution. All solutions were checked for the absence of free Gd(III) ion using the xylenol orange test [28]. Final concentrations of 0.5mM were prepared in 1:1 (V/V) glycerol/water solution. The glasses were formed by flash freezing the sample in liquid nitrogen before loading into the pre-cooled continuous-flow cryostat.

The magnetically dilute powders were prepared from a solution of 99% of $Y(ClO_4)_3$ / 1% of $Gd(ClO_4)_3$ and DTPA and DOTA ligands. The samples were lyophilized using a Speed Vac Concentrator. The solids obtained were finely ground in order to obtain a homogenous powder. Gd-P792(B) and Gd-P792(R) [29] powders were used without any spin dilution, because the dipolar interactions between gadolinium ions are small in this case due to the important molecular size of both Gd-P792 compounds.

3. *EPR Measurements*. The EPR spectra at 240 GHz were measured at the EPR facility of the National High Magnetic Field Laboratory with a home-built quasi-optical superheterodyne spectrometer [30]. A configuration without cavity was used, with a teflon sample cup containing the powders. The photon energy of 240 GHz electromagnetic radiation corresponds to a temperature of 11.5 K. Therefore, at 4 K almost only the transitions between the lowest energy levels are observed. However, even at a very low irradiation power with a B_1 field smaller than 1 μT, the spectrum was distorted due to saturation. For that reason, at the lowest temperatures, rapid-passage EPR [31] was employed to record

the spectra, using relatively high power (~ 1mW at the sample, B_1 ~ 10 μT) and small modulation amplitudes. Instead of a derivative lineshape, the absorption lineshape is directly obtained. At temperatures above 30 K, standard CW-EPR was used. Lower frequencies EPR spectra were recorded at X-band (9.44 GHz) and Q-band (~34 GHz) on a Bruker ELEXSYS E 500 spectrometer. CW-EPR was used at all frequencies.

4. *Data Analysis.* The EPR spectra were simulated and fitted using a home-written program EPRcalc [32],[29] which utilises complete diagonalization of the effective spin Hamiltonian, which can be written as follows:

$$\hat{H} = \mu_B \hat{S} \cdot \vec{\vec{g}} \cdot \vec{B} + D(\hat{S}_z^2 - \hat{S}^2/3) + E(\hat{S}_x^2 - \hat{S}_y^2) \quad (1)$$

with S=7/2. The first term represents the field dependent electron Zeeman contribution and the second and third terms, without any explicit B_0-dependence, represent the zero-field splitting. The parameter $\vec{\vec{g}}$ is the Zeeman splitting tensor, μ_B the Bohr magneton, and B_0 the external magnetic field. D and E are the axial and rhombic ZFS coefficients, which describe the deviation from the octahedral and the axial symmetry, respectively.

The distributions, in the frozen solution and the powders, of D and E are noted D-strain (σD) and E-strain (σE) and are assumed to be Gaussian and given by:

$$P(D_i) \sim e^{-\left(\frac{2(D_i - D)}{\sigma D}\right)^2}; \qquad P(E_i) \sim e^{-\left(\frac{2(E_i - E)}{\sigma E}\right)^2} \quad (2)$$

They are accounted for by including a Gaussian line-broadening that is proportional to the shift of the transitions due to a change in D and E. No correlation between σD and σE is assumed.

Higher order terms in the ZFS and the terms arising from the nuclear interactions - nuclear hyperfine, nuclear Zeeman, superhyperfine, and quadrupole interactions - are neglected.

Results and Discussion. - As it was underlined in the previous EPR study of Gd(III) complexes in frozen solutions (glasses) [27], recording EPR spectra at 240 GHz and very low temperatures (below 150 K) allows a direct and straightforward determination of the parameters governing the strength of ZFS. Furthermore, it provided us with an elegant way to determine the sign of the axial ZFS parameter

D. A correlation has been established between the sign of *D*, and the nature of the chelating ligand in the studied Gd(III) complexes: positive and negative signs have been observed for acyclic (e.g. DTPA) and marcocyclic (e.g. DOTA) complexes, respectively. *Fig. 1* [27] shows experimental and calculated EPR spectra of $[Gd(DTPA)(H_2O)]^{2-}$ and $[Gd(DOTA)(H_2O)]^{-}$ glasses at 240 GHz and 4 K. The sign of D is unequivocally defined by the small, narrow peak due to the $-1/2 \rightarrow +1/2$ transition being at lower or higher field with respect to the maximum of the broad peak which at 4K is mainly due to the $-7/2 \rightarrow -5/2$ transition. The four ZFS parameters *D*, *E*, σD and σE were determined from least square fitting of 4 K spectra. The validity of the fitted ZFS parameters was then confirmed by their ability to simulate the higher temperature spectra at 240 GHz [27].

1. *Frozen solutions*. In the aim to assess the soundness of the high frequency results, further measurements and simulations for $[Gd(DTPA)(H_2O)]^{2-}$ and $[Gd(DOTA)(H_2O)]^{-}$ glasses were carried out at Q-band and X-band. *Fig. 2* illustrates experimental and simulated spectra obtained with the high field parameters of both complexes at these two bands at 160 K. Fitting the Q-band spectra by adjusting *D*, *E*, σD and σE leads only to a slight improvement of the agreement between the calculated and the experimental spectra and the parameters obtained change less than 10%. However, using these fitted parameters to simulate the 240 GHz and 4K data led to noticeable disagreement between the calculated and the experimental spectra. Therefore, we report only the spectra simulated at Q- and X-band with the 240 GHz and 4K parameters defined previously [27] (*Table 1*). A fit of the spectra at X-band was not possible because the approximation used to calculate the strain break down if the ZFS parameters are of the same order of magnitude as the observation frequency.

The comparison among spectra at different frequencies reveals certain important trends. At 240 GHz (*Fig. 1*), the $[Gd(DTPA)(H_2O)]^{2-}$ spectrum is about two times broader than that of $[Gd(DOTA)(H_2O)]^{-}$, a tendency which is retained at lower frequencies. Complex spectral features are observed at X-band and to a minor extent at Q-band for $[Gd(DTPA)(H_2O)]^{2-}$. In the simulations, these features are highly sensitive to changes in the ZFS parameters, especially *D*. For $[Gd(DOTA)(H_2O)]^{-}$, the spectra at Q- and X-band exhibit only small satellite peaks around one main sharp peak (*Fig. 2*).

These spectra are less informative than the one obtained at 240 GHz. The difference in the apparent spectral width and the spectral complexity can be essentially explained by the larger magnitude of the ZFS parameter D for the acyclic $[Gd(DTPA)(H_2O)]^{2-}$ compared to the cyclic $[Gd(DOTA)(H_2O)]^{-}$.

2. *Powders.* EPR spectra of magnetically dilute powders of $[Y(DTPA)(H_2O)]^{2-}$ and $[Y(DOTA)(H_2O)]^{-}$ with ~1%(w/w) of Gd(III) ion have been measured at 240 GHz, Q- and X-band from 5 K to 298 K (*Figs. 3, 4*). The high frequency and low temperature powder spectra have been fitted using the same procedure as for the frozen solutions by adjusting the four ZFS parameters D, E, σD and σE. Spectra measured at Q- and X-bands and at 298 K have only been simulated and are represented in *Fig. 4*. The fitted parameters are reported in *Table 1*. The agreement of the fit to the experimental data is not as good for the powders as for the frozen solutions. This is likely due to a non-Gaussian distribution of D and E values is the powder.

The results show that the sign of D calculated from 4-5K and 240 GHz spectra for both complexes is the opposite of the one obtained from glasses, a fact that can already be observed by comparing the spectra of glasses and powders (*Figs. 1-3*). The magnitudes of the ZFS parameters for the powders are also different from those obtained in frozen solutions [27]. A change in value of D and E is indicative of differences in the structure around the paramagnetic center. In the case of our powders, we observe a ZFS strain which is of the same magnitude as the average ZFS itself. The strain is often interpreted in terms of distribution of hydrogen bonding throughout a disordered sample, yielding slightly different charges densities around each paramagnetic center [26]. Therefore, even small changes in the vicinity of the chelate molecules could lead to significant changes in D and E, including a shift of its average values. In particular, when studying powders instead of liquid or frozen solutions, the replacement of well organized second shell water molecules by counter ions and/or the small excess of free ligand molecules could explain the observed changes between the measured powders and frozen solutions spectra and thus the calculated parameters.

Contrary to our working hypothesis, the magnitude of the transient ZFS parameters σD and σE remains significant in powders especially for the DOTA complex (*Table 1*). This could be a

consequence of the sample preparation. The liophilization procedure used may hinder the formation of ordered unit cells. In addition the slight excess of ligand molecules can induce disorder in the final solid, leading to a distribution of ZFS parameters.

As it was described in previous studies, the transient ZFS modulation can be regarded as a dynamic equivalent of the strain observed in powders and frozen solutions [33]. Using the current definition of the strain parameters (full width at 0.6065 height of the Gaussian distribution), the transient ZFS strength in Rast's approach, a_{2T}, is given as

$$a_{2T} = [2/3(\sigma D/2)^2 + 2(\sigma E/2)^2]^{1/2} \quad (3)$$

Similarly, the second order term parameter of the static ZFS strengths, a_2, is given by:

$$a_2 = [2/3D^2 + 2E^2]^{1/2} \quad (4)$$

It is now possible to compare values of a_2 and a_{2T} measured for $[Gd(DTPA)H_2O]^{2-}$ and $[Gd(DOTA)\ H_2O]^-$ in powders, glasses and liquid solution (*Table 2*). For both complexes a_2 calculated from the glassy samples is similar to that obtained from relaxation studies in aqueous solution [11, 27]. However, the calculated static and transient ZFS in powders are significantly different. Thus, we show that the determination of ZFS parameters in glassy samples yields results more relevant to the problem of electron spin relaxation in aqueous solution than those obtained in powders. This finding is quite reasonable if we consider that the environment of the Gd(III) complexes in frozen water/glycerol mixtures is much closer to that in an aqueous solution than that of powders.

EPR spectra of powders of the macromolecular DOTA-derivative in its isomeric pure form P792 (B) and in mixture of six isomers (R) have been measured at 240 GHz, Q- and X-band from 5 K to 298 K. Experimental and fitted spectra of both compounds in frozen solutions and powders are compared in *Fig. 5*. As for powders of DTPA- and DOTA- complexes, high frequency-low temperature spectra have been fitted by adjusting the four ZFS parameters D, E, σD and σE (*Table 3*). Experimental and simulated spectra at Q- and X-band and 298K are presented in *Fig. 6*. In contrast to what we observed for the DOTA complex, no broadening of the spectra at 240 GHz and 4 K is noticeable in powders of both macromolecular complexes reflecting a minimal change in the magnitude of D values. However,

for both complexes the sign of D is the opposite in powders as compared to glasses, indicating a change in structure, similar to that observed for $[Gd(DOTA)(H_2O)]^-$. Again, this sign change appears unambiguously in the experimental spectra at high frequency and low temperature (*Fig. 5*). The values of the strain σD and σE are in powders as large as in frozen solutions. Powders of the Gd-P792 complexes were also prepared by the liophilization procedure, and as it was mentioned for the DTPA- and DOTA- complexes, the large values of strain could be attributed to the sample preparation.

Our results show that powders of Gd(III) complexes with cyclic ligands prepared by a liophilization procedure suffer from disorder similar to frozen solutions. Because this disorder is reflected by relatively large values of σD and σE, determination of axial and rhombic parameters D and E is not easier than in glasses. Together with the small environment changes described above it follows that experiments on powders of DOTA and DOTA-derivative complexes show no additional advantages compared to those on frozen solution.

Finally, we shortly discuss a possible extension of this work to further simplify the analysis. Spectra of single crystals should in principle lack both structural disorder and angular distribution and therefore allow to remove one more level of disorder from the sample. Thus, they offer an attractive route towards a precise, unambiguous determination of the static ZFS parameters D and E, as well as higher order terms. However, our results with powders suggest that such parameters might not be useful from the point of view of relaxation in liquids. Single crystal results besides the difficulty to obtain single crystals are even more likely to suffer from structural differences compared to frozen and liquid solutions.

Conclusions. - Many Gd(III) based contrast agents for MRI have significant static ZFS which has a non negligible influence on the electronic relaxation of these compounds. The understanding of the origin of both the transient and the static ZFS, will help to explain the relaxivity of Gd(III) complexes relevant as contrast agents for MRI. A first step towards this aim was accomplished thanks to the direct determination of ZFS through performing high field / high frequency EPR measurements for several Gd(III) complexes in frozen solution. The static ZFS parameters in frozen solution were shown to be in

good agreement with those obtained in aqueous solution. Lower frequencies (X- and Q- band) measurement and spectral simulations for $[Gd(DTPA)(H_2O)]^{2-}$ and $[Gd(DOTA)(H_2O)]^{-}$ confirmed the soundness of the high frequency results.

Contrary to what we expected, powder samples do not allow a more precise determination of the static ZFS parameters (D, E) by reducing the strain (σD, σE) due to disorder. EPR experiments at multiple frequencies and variable temperature were performed on magnetically dilute $[Gd(DTPA)(H_2O)]^{2-}$, $[Gd(DOTA)(H_2O)]^{-}$ and the macromolecular DOTA-derivative Gd-P792(R/B), and showed that substantial disorder is present in the powders obtained by liophilization. Furthermore, we observe significant differences on the ZFS of our powders compared to the frozen solutions, even including a systematic sign reversal of D. The main conclusion for both frozen solutions and powders is that the results obtained in glasses are more relevant to the problem of electron spin relaxation in aqueous solution. Finally, high field EPR technique combined with very low temperature in frozen solution turned out to be the more appropriate technique to determine accurately the magnitude of the ZFS parameters and more specifically the sign of the axial ZFS parameter D.

The authors are grateful to the Program Enhancement Grant 01-05 from the FSU Foundation to the NHMFL EMR program for financial support. This work has been supported by the Swiss National Science Foundation and the Swiss state Secretariat for Education and Research (SER). This research was carried out in the frame of the EU COST Action D38 and European founded EMIL program LSHC-2004-503569. We are grateful to Dr. Cyrille Denarie (EPFL) for his help with the liophilization procedure.

Tables

Table 1. The ZFS parameters obtained by fitting the experimental EPR spectra at 240 GHz of glasses (4K) and powders (5K) for $[Gd(DTPA)H_2O]^{2-}$ and $[Gd(DOTA)H_2O]^{-}$ Estimated error is equal to 0.002 cm^{-1}

	$[Gd(DTPA)(H_2O)]^{2-}$		$[Gd(DOTA)(H_2O)]^{-}$	
	powder	glass[a])	powder	glass[a])
D (cm^{-1})	-0.029	0.048	0.030	-0.019
E (cm^{-1})	0.004	0.013	0.006	0.000
E/D	-0.14	0.27	0.20	0.00
σD (cm^{-1})	0.005	0.022	0.026	0.019
σE (cm^{-1})	0.001	0.007	0.004	0.013

[a]) ref. [27].

Table 2. The ZFS parameters determined by Rast method in solution in comparison with the parameters obtained from glasses and powders for $[Gd(DTPA)H_2O]^{2-}$ and $[Gd(DOTA)H_2O]^{-}$

	$[Gd(DTPA)(H_2O)]^{2-}$			$[Gd(DOTA)(H_2O)]^{-}$		
	powder this work	frozen solution[a])	aqueous solution[b])	powder this work	frozen solution[a])	aqueous solution[b])
$a_2/10^{10}$ s^{-1}	0.46	0.80	0.92	0.49	0.30	0.35
$a_{2T}/10^{10}$ s^{-1}	0.04	0.22	0.43	0.20	0.23	0.43

[a]) ref. [27]. [b]) ref. [9]

Table 3. The ZFS parameters obtained by fitting the experimental EPR spectra at 4 K and 240 GHz of Gd-P792. Estimated error is equal to 0.002 cm^{-1}

	Gd-P792(B)		Gd-P792(R)	
	powder	glass[a])	powder	glass[a])
D (cm^{-1})	0.055	-0.060	-0.035	0.033
E (cm^{-1})	0.011	0.000	0.010	0.010
E/D	0.20	0.00	-0.26	0.30
σD (cm^{-1})	0.045	0.060	0.029	0.016
σE (cm^{-1})	0.023	0.010	0.013	0.013

[a]) ref. [27].

SCHEME TITLE

Molecular structure of $[Gd(DTPA)(H_2O)]^{2-}$, $[Gd(DOTA)(H_2O)]^{-}$ and Gd-P792(B/R)

FIGURE CAPTIONS

Fig. 1. Experimental (upper) *and fitted* (lower) *EPR spectra in water-glycerol glasses at 240 GHz for* $[Gd(DTPA)(H_2O)]^{2-}$ (left) *and* $[Gd(DOTA)(H_2O)]^{-}$ (right) (taken from [27]).

Fig. 2. Experimental (upper) *and simulated* (lower) EPR *spectra in water-glycerol glasses at* (a) Q-*band,* (b) *X-band for* $[Gd(DTPA)(H_2O)]^{2-}$ (left) *and* $[Gd(DOTA)(H_2O)]^{-}$ (right).

Fig. 3. Experimental (upper) *and fitted* (lower) *EPR spectra of magnetically dilute powders with* ~1%(w/w) *Gd(III) at 240 GHz for* $[Y(DTPA)(H_2O)]^{2-}$ (left) *and* $[Y(DOTA)(H_2O)]^{-}$ (right).

Fig. 4. Experimental (upper) *and simulated* (lower) *EPR spectra of magnetically dilute powders with ~1%(w/w) Gd(III) at* (a) *Q-band,* (b) *X-band for* $[Y(DTPA)(H_2O)]^{2-}$ (left) *and* $[Y(DOTA)(H_2O)]^{-}$ (right).

Fig. 5. Experimental (upper) *and fitte*d (lower) *EPR spectra at 240 GHz for* (a) *Gd-P792 glasses,* (b) *Gd-P792 powders: Gd-P792(B)* (left) *and Gd-P792(R) (*right).

Fig. 6. Experimental (upper) *and simulated* (lower) *EPR spectra of Gd-P792 powders at* (a) *Q-band,* (b) X-*band: Gd-P792(B)* (left) and *Gd-P792(R)* (right).

Scheme.

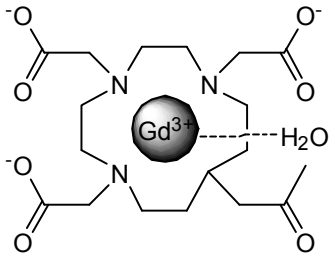

$[Gd(DOTA)(H_2O)]^-$

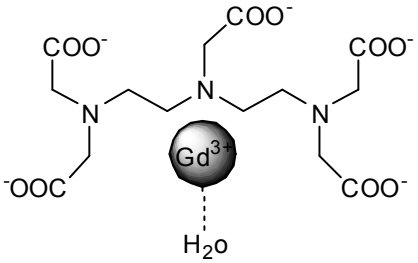

$[Gd(DTPA)(H_2O)]^{2-}$

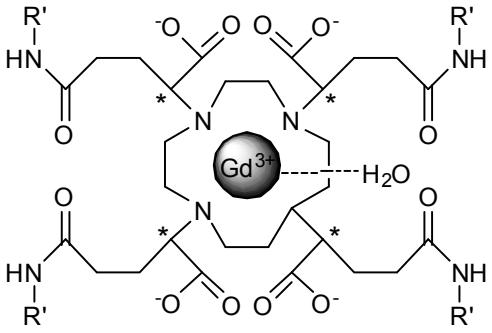

Gd-P792(R) - Gd-P792(B)

R' =

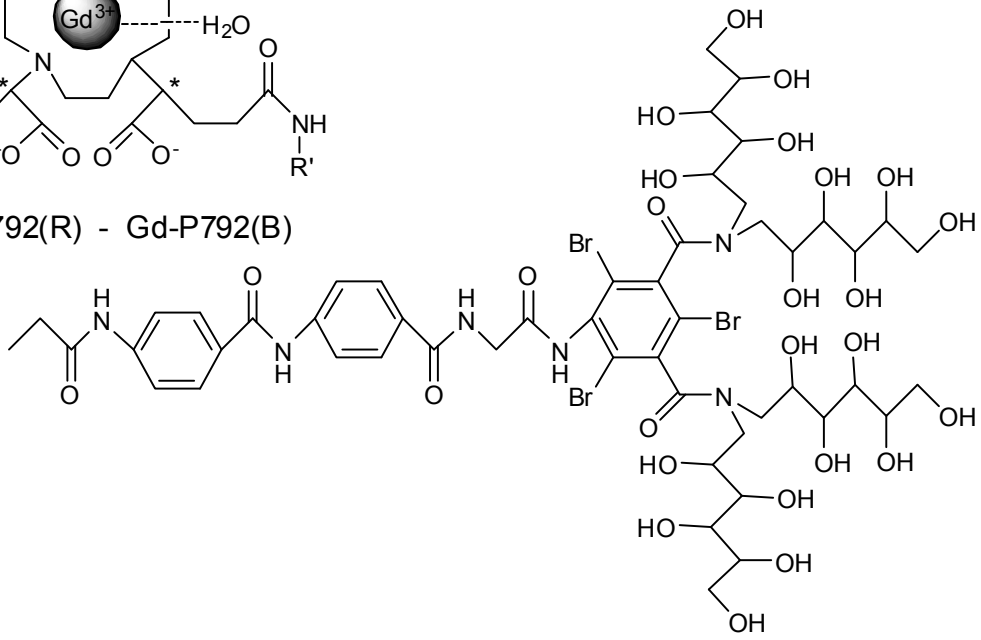

Figure 1

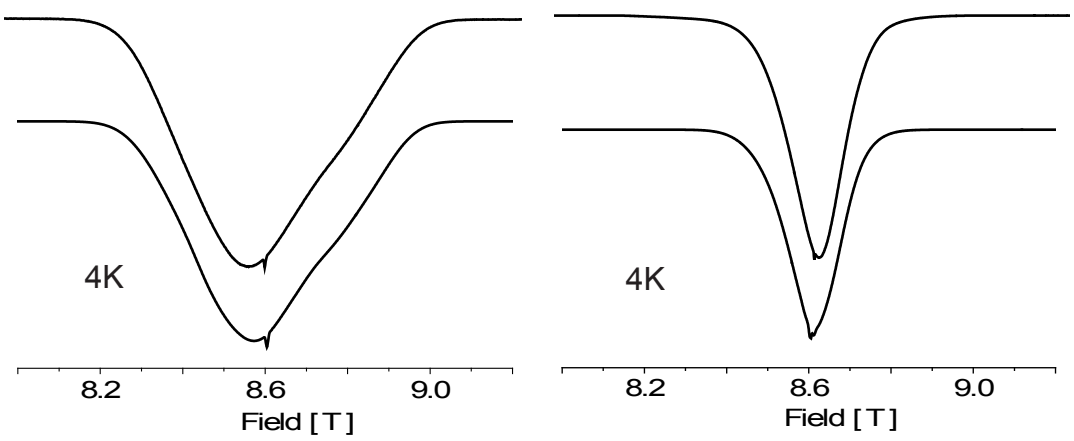

Figure 2

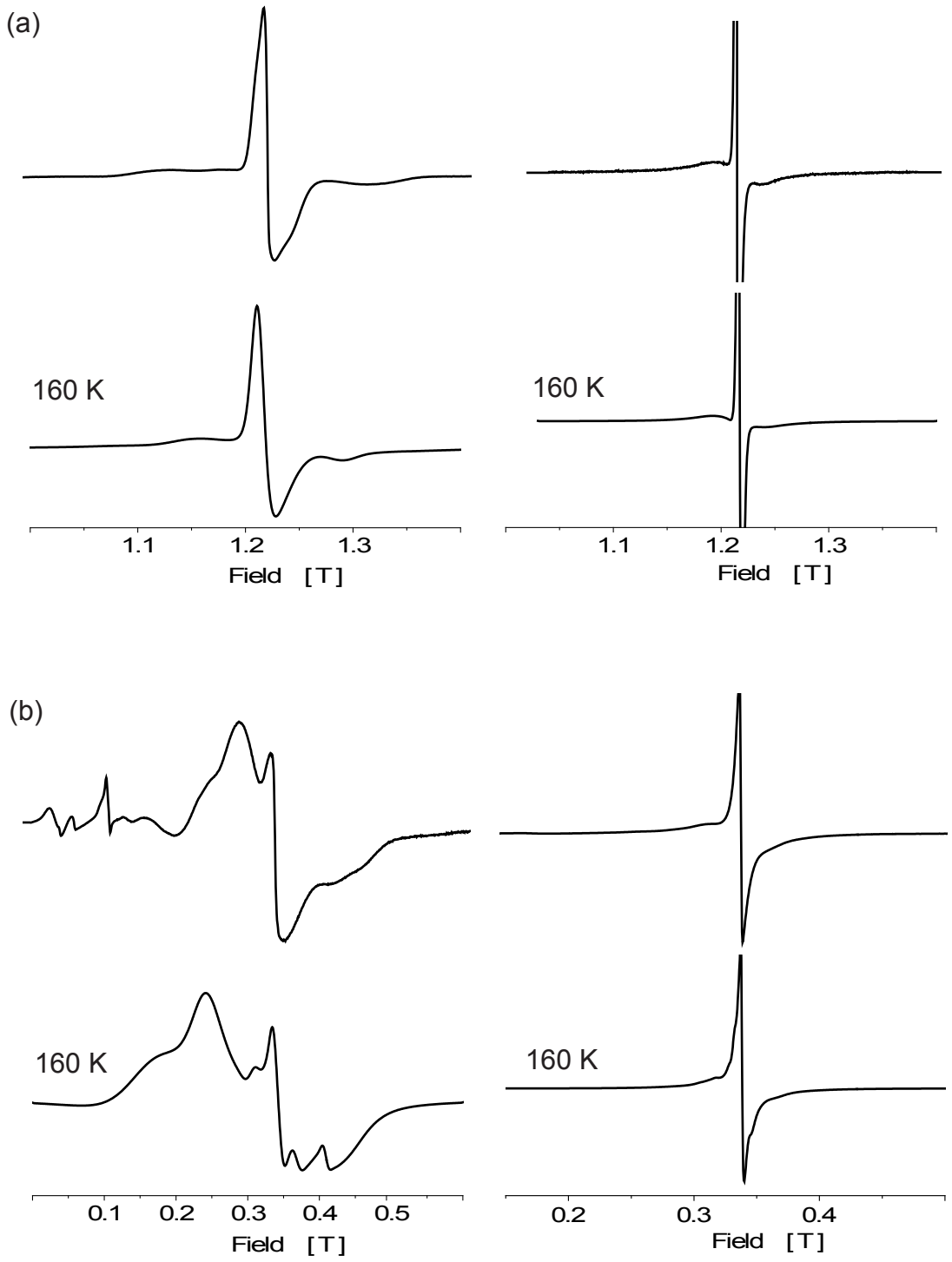
(a)
160 K
1.1
1.2
1.3
Field [T]
160 K
1.1
1.2
1.3
Field [T]
(b)
160 K
0.1
0.2
0.3
0.4
0.5
Field [T]
160 K
0.2
0.3
0.4
Field [T]

Figure 3

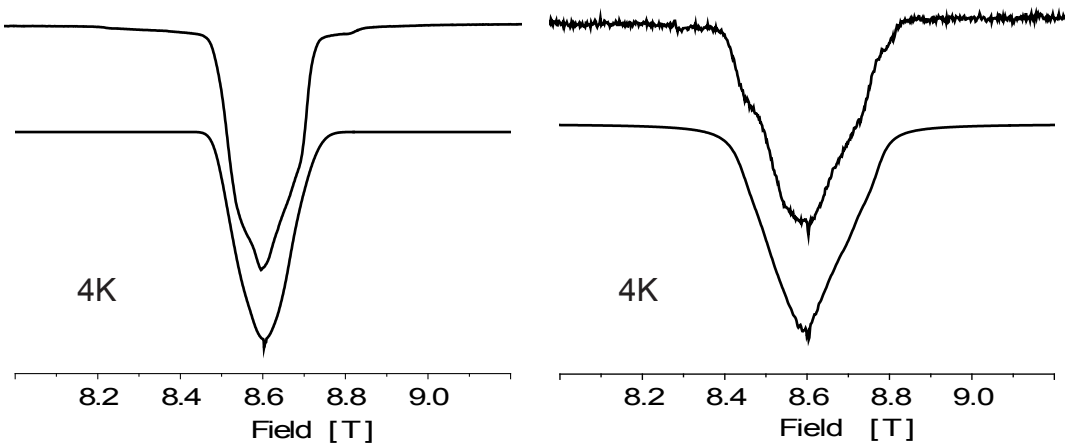

Figure 4

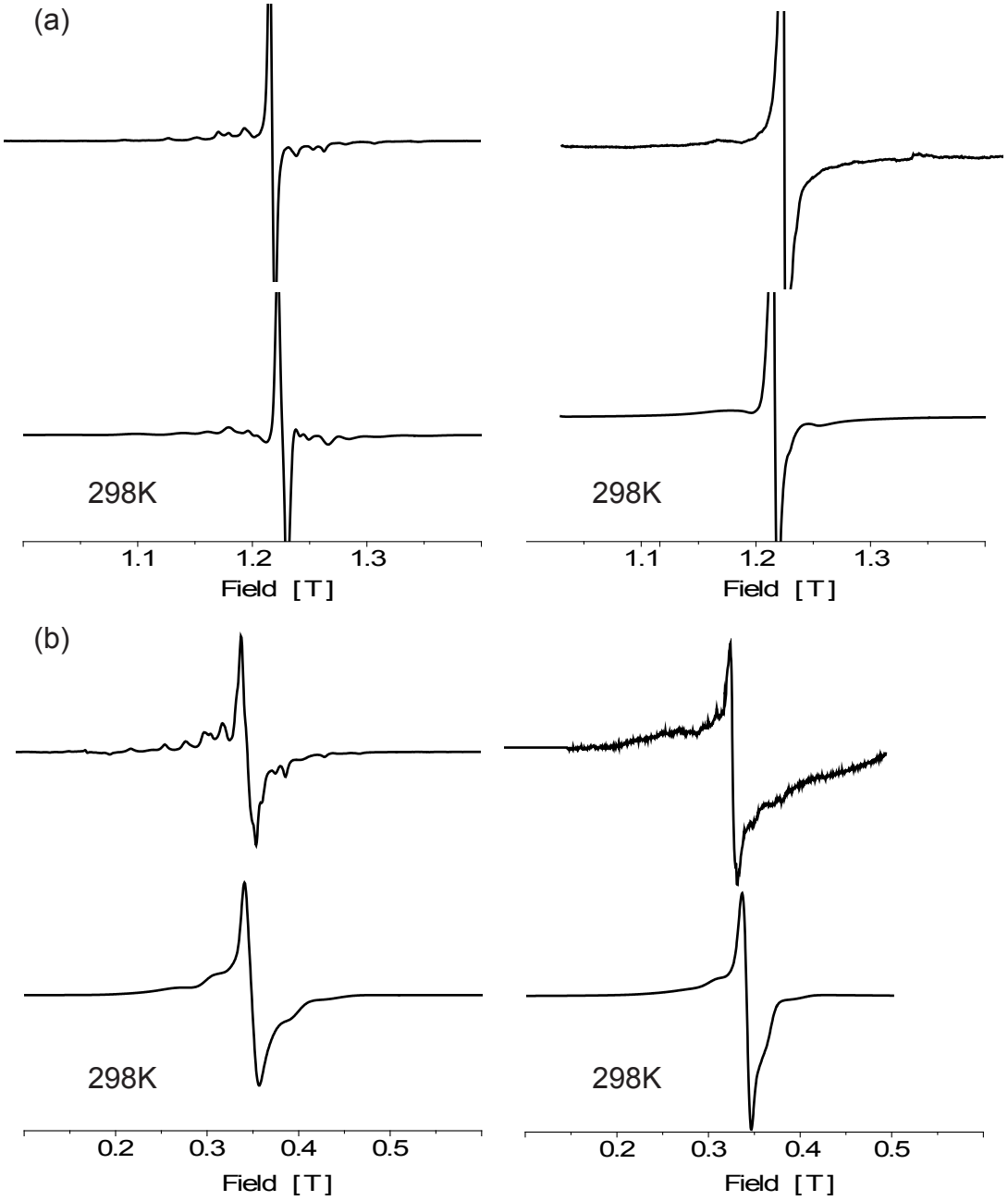
(a)
298K
1.1
1.2
1.3
Field [T]
298K
1.1
1.2
1.3
Field [T]
(b)
298K
0.2
0.3
0.4
0.5
Field [T]
298K
0.2
0.3
0.4
0.5
Field [T]

Figure 5

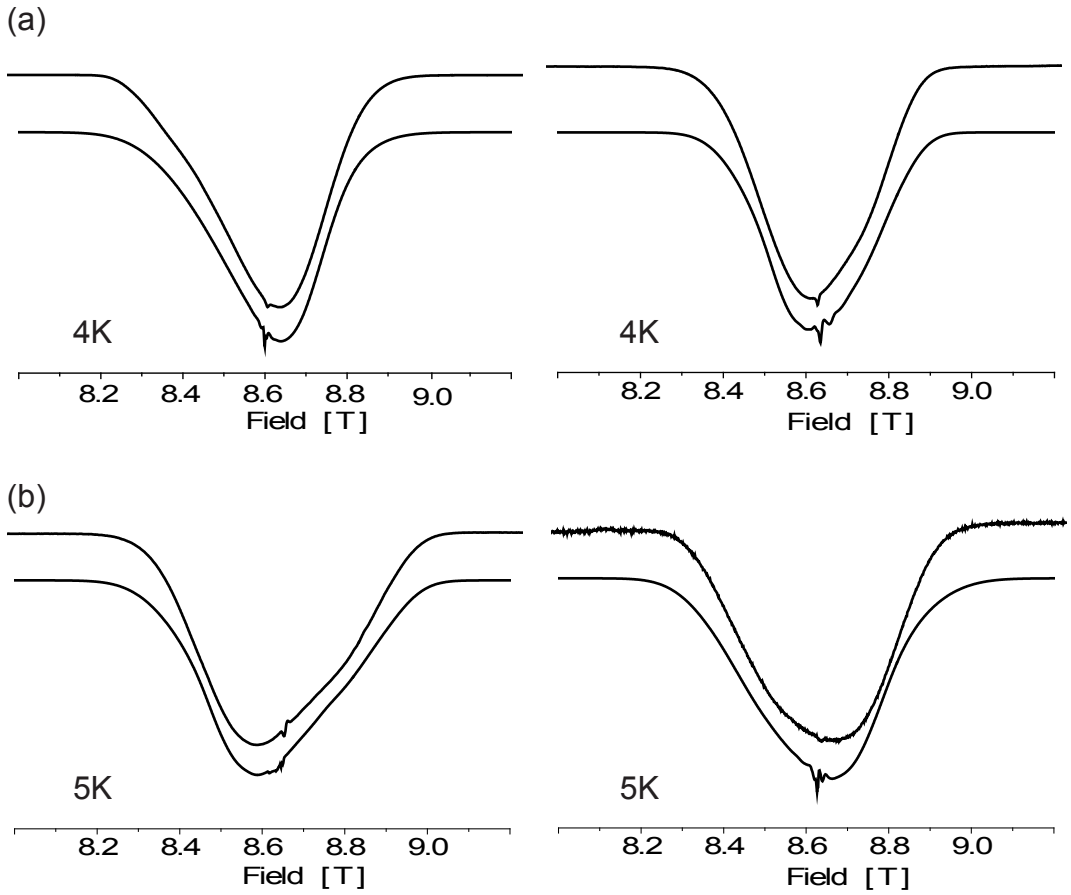
(a)
4K
8.2
8.4
8.6
8.8
9.0
Field [T]
4K
8.2
8.4
8.6
8.8
9.0
Field [T]
(b)
5K
8.2
8.4
8.6
8.8
9.0
Field [T]
5K
8.2
8.4
8.6
8.8
9.0
Field [T]

Figure 6

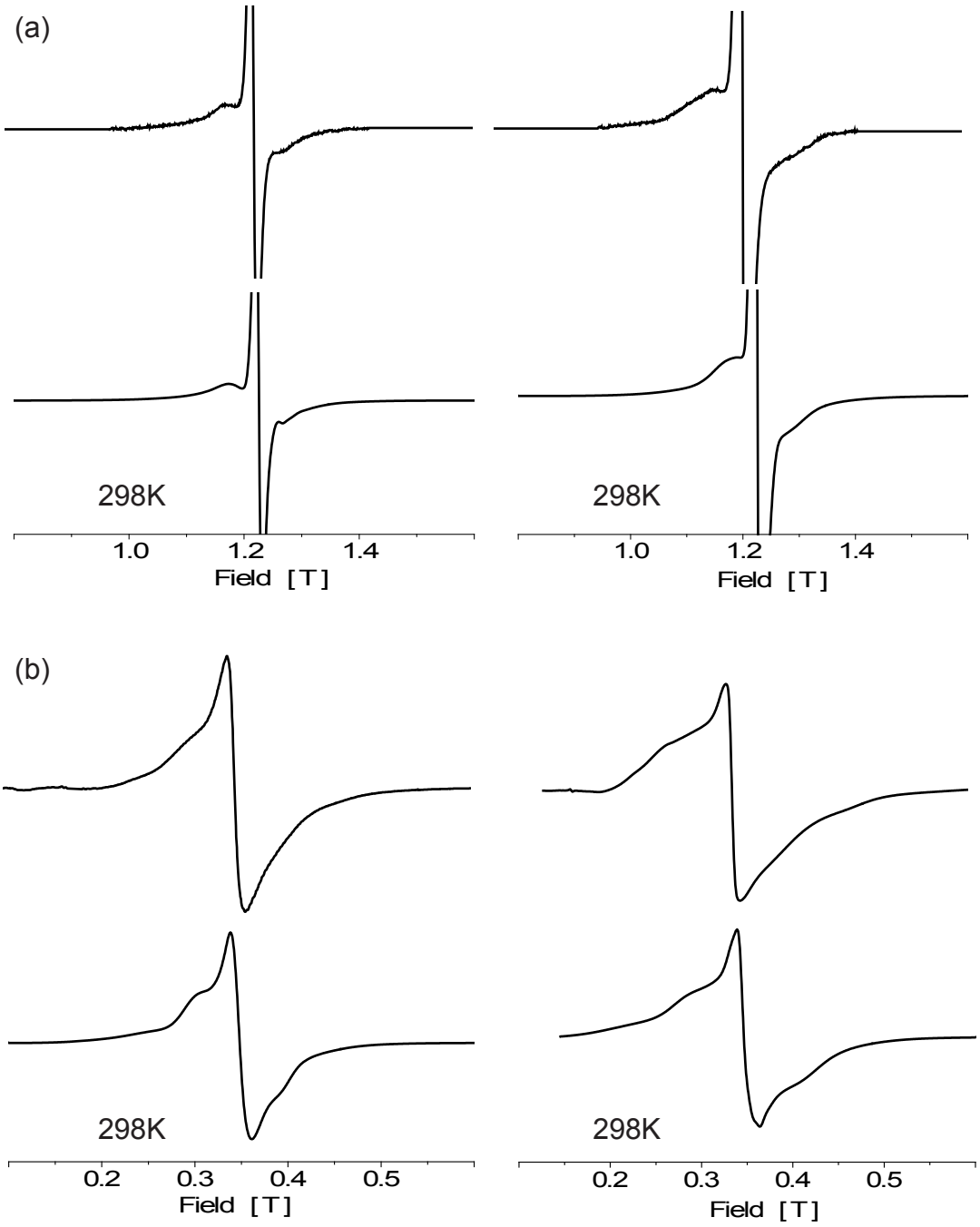
(a)
298K
1.0
1.2
1.4
Field [T]
298K
1.0
1.2
1.4
Field [T]
(b)
298K
0.2
0.3
0.4
0.5
Field [T]
298K
0.2
0.3
0.4
0.5
Field [T]

REFERENCES

[1] A. E. Merbach, É. Tóth, " The Chemistry of Contrast Agents in Medical Magnetic Resonance Imaging", 1st ed., John Wiley & Sons, Chichester, **2001**, p. 471.
[2] P. Caravan, J. J. Ellison, T. J. McMurry, R. B. Lauffer, *Chem. Rev.* **1999**, *99*, 2293.
[3] G. M. Nicolle, É. Tóth, K.-P. Eisenwiener, H. R. Mäcke, A. E. Merbach, *J. Biol. Inorg. Chem.* **2002**, *7*, 757.
[4] L. Helm, A. E. Merbach, *Chem. Rev.* **2005**, *105*, 1923.
[5] Z. Jászberényi, A. Sour, É. Tóth, M. Benmelouka, A. E. Merbach, *Dalton Trans.* **2005**, 2713.
[6] E. Strandberg, P.-O. Westlund, *J. Magn. Reson. A* **1996**, *122*, 179.
[7] R. B. Clarkson, A. I. Smirnov, T. I. Smirnova, H. Kang, R. L. Belford, K. Earle, J. H. Freed, *Mol. Phys.* **1998**, *95*, 1325.
[8] S. Rast, P. H. Fries, E. Belorizky, *J. Chem. Phys.* **2000**, *113*, 8724.
[9] S. Rast, A. Borel, L. Helm, E. Belorizky, P. H. Fries, A. E. Merbach, *J. Am. Chem. Soc.* **2001**, *123*, 2637.
[10] T. Nilsson, J. Kowalewski, *Mol. Phys.* **2000**, *98*, 1617.
[11] S. Rast, P. H. Fries, E. Belorizky, A. Borel, L. Helm, A. E. Merbach, *J. Chem. Phys.* **2001**, *115*, 7554.
[12] D. Kruk, T. Nilsson, J. Kowalewski, *Phys. Chem. Chem. Phys.* **2001**, *3*, 4907.
[13] M. Benmelouka, A. Borel, L. Moriggi, L. Helm , A. E. Merbach, *J. Phys. Chem. B* **2007**, *111*, 832.
[14] A. Borel, J. F. Bean, R. B. Clarkson, L. Helm, L. Moriggi, A. D. Sherry, M. Woods, *Chem. Eur. J.* **2008**, *14*, 2658.
[15] E. Belorizky, P. H. Fries, L. Helm, J. Kowalewski, D. Kruk, R. R. Sharp, P.-O. Westlund, *J. Chem. Phys.* **2008**, *128*, 052307.
[16] G. E. Uhlenbeck, L. S. Ornstein, *Phys. Rev.* **1930**, *36*, 823.
[17] W. Froncisz, J. S. Hyde, *J. Chem. Phys* **1980**, *73*, 3123.
[18] W. R. Hagen, D. O. Hearshen, R. H. Sands, W. R. Dunham, *J. Magn. Res.* **1985**, *61*, 220.
[19] B. Cage, A. K. Hassan, L. Pardi, J. Krzystek, L.-C. Brunel, N. S. Dalal, *J. Magn. Res. A* **1997**, *124*, 495.
[20] D. Mustafi, E. V. Galtseva, J. Krystek, L.-C. Brunel, M. W. Makinen, *J. Phys. Chem. A* **1999**, *103*, 11279.
[21] G. Lassmann, M. Kolberg, G. Bleifuss, A. Graslund, B. M. Sjoberg, W. Lubitz, *Phys. Chem. Chem. Phys.* **2003**, *5*, 2442.
[22] S. Cannistraro, *J. Phys. France* **1990**, *51*, 131.
[23] A. Venturelli, M. A. Nilges, A. Smirnov, R. L. Belford, L. C. Francesconi, *J. Chem. Soc. Dalton Trans.* **1999**, 301.
[24] G. N. George, R. C. Prince, R. E. Bare, *Inorg. Chem.* **1996**, *35*, 434.
[25] A. J. Pierik, W. R. Hagen, W. R. Dunham, R. H. Sands, *Eur. J. Biochem.* **1992**, *206*, 705.
[26] A. Seidel, H. Bill E., L., P. Nordblad, F. Kilar, *Arch. Biochem. Biophys.* **1994**, *308*, 52.
[27] M. Benmelouka, J. Van Tol, A. Borel, M. Port, L. Helm, L. C. Brunel, A. E. Merbach, *J. Am. Chem. Soc.* **2006**, *128*, 7808.
[28] M. Randin, G. Brunisholz, *Helv. Chim. Acta* **1959**, *42*, 1927.
[29] M. Port, C. Corot, O. Rousseaux, I. Raynal, L. Devoldere, J. M. Idée, A. Dencausse, *Magn. Reson. Matter. Phys. Biol. Med.* **2001**, *12*, 121.
[30] J. van Tol, L.-C. Brunel, R. J. Wylde, *Rev. Sci. Instrum.* **2005**, *76*, 74101.
[31] A. M. Portis, *Phys. Rev.* **1955**, *100*, 1219.
[32] J. Van Tol, National High Magnetic Field Laboratory, **2005**.
[33] A. Borel, R. B. Clarkson, R. L. Belford, *J. Chem. Soc.* **2007**, *126*, 054510.